IMPROVEMENT THE ROOT STABILITY OF THICK WELDS DURING ELECTRON BEAM WELDING

Petr HAVLÍK [1], Jan KOUŘIL [1], Ivo DLOUHÝ [1]

[1]*Institute of Materials Science and Engineering, NETME center, Brno University of technology, Technická 2896/2, 616 69 Brno, Czech Republic, EU, havlik03pet@rmail.com*

Abstract

Electron beam (EB) welding of thick materials is not an easy task and finding the correct welding parameters and conditions is one of the crucial factors especially when the quality of weld root is required. The undesirable features of an electron beam weld can lead to premature failure or reduces the effectiveness of the resulting components (for example impellers). In attempts to understand how these defects are formed, the formation of EB cavity is primary importance. The greatest significance is attributed to the cavity oscillation in size and shape due to the rapid pressure and temperature changes which occurs during formation of EB cavity. These dynamic behaviors of molten metal during EBW enable creation of liquid metal protrusions in cavity instabilities - spiking. In the preset paper the initial results of several steel and titanium plates with different thickness welded without filler metal are presented. During the welding various approaches have been verified to eliminating the spiking. For spiking elimination the modification of weld joint configuration was tested, using of solder, using of background material and modification of EB welding process parameters. The obtained results are complemented by microstructure analysis and by evaluation of the quality and appearance of the weld root.

Keywords: Electron beam welding, spiking, steel, titanium alloy, thick welds

1. INTRODUCTION

The deep welding capability of an electron beam has been well publicized by equipment manufactures as well as researchers. The reason why the welds with the high ratio of depth-to-width of fusion zone are created during EB welding, is the presence of cavity in the path of EB. Vapour pressure of the elements in the materials being welded, plays an important role in maintaining a weld-cavity keyhole. However, a very important additional force tending to close the cavity is due to the surface tension. During the depth penetration welding, the cavity is assumed to resemble a deep and narrow depression with liquid walls, and the force of gravity acting on the liquid metal in the keyhole may not overcome the surface tension forces when welding in vertical position. The undesirable features of EB welds, such as spikes, cold shuts and base porosity may occur. These defects seriously reduce the properties and strength of the joint [1,2]. Spiking represents unexpected increase in the local penetration in periodic successions. Different mechanisms of spiking have been proposed in literature. Tong and Giedt [1] proposed that spiking formed from the oscillation of the keyhole were produced during keyhole mode EB welding. The severity of spiking thus depended on the frequency of the oscillation of the cavity, welding speed, and the material to be welded. Armstrong [3] suggested that spiking was determined by power density and beam power. Arata et al. [4] observed spiking formation during the breakdown of force balance between vapor pressure, hydrostatic pressure, and dynamic force of liquid layer. Based on these results Giedt [5] suggested for partial penetration welds that the depth of a spike is proportional to the melting distance in a time scale, which equals the energy distribution parameter (described by used size of EB spot) divided by welding speed. Wei et al. [6] introducing a melting efficiency and energy for melting. The spiking amplitude-to-average fusion zone depth ratio is proportional to the width of the fusion zone divided by multiple of melting efficiency with size of EB spot in welding direction.

The objective of the present study was to reduce of spiking in full penetration EB welds. For spiking elimination were tested several approaches which include the modification of weld joint configuration, using of background material with a different chemical composition than base metals, using of solder and modification of the process parameters.

2. EXPERIMENTAL MATERIALS AND PORCEDURES

Experimental thick welds were welded by universal chamber electron beam machine Pro-Beam (Germany) K26 EBG 60-150. For experimental works were used precipitation hardening martensitic stainless steel X5CrNiCuNb16-4 (referred as to X5; samples S1 - S7) in solution annealed condition and titanium alloy Ti-6Al-4V (referred as to Ti64; samples T1 - T5). The chemical composition of base metals (BM) was given in **Table 1**. For determine of the average chemical composition of X5 steel was used the emission spectrometer with glow discharge Spectrumat GDS 750. Chemical composition of Ti64 have been taken from a copy of the "inspection Certificate" (VSMPO-AVISMA Corporation, Russia). During individual test the butt welds were welded with thickness t = 10 and 20 mm.

Table 1 Chemical composition of X5 steel and Ti64 alloy (in wt. %).

Material	C	Mn	Si	Cr	Ni	Mo	Cu	Nb	Fe
X5	0.03	0.60	0.38	15.47	4.13	0.11	4.27	0.25	balance
	Al	**V**	**Fe**	**O**	**C**	**N**	**H**	**Ti**	
Ti64	6.46	4.11	0.21	0.17	0.007	0.004	0.006	balance	

Experimental was divided in four stages: in the first stage was evaluated the weldability of BM; in the second stage were used background materials in order to avoid excessive projections of weld metal (WM): tungsten electrode WL10 (doped by 0.90 - 1.20 wt. % La_2O_3 [7]) and nickel solder BNi-7 filling the root gap. Chemical composition of used solder was: 14.00 wt. % Cr; 10.10 wt. % P; 0.06 wt. % C and 75.84 wt. % Ni. During welding with solder was used the insufficient beam energy. It was expected, that a solder was should melted by heat dissipation. The third stage was focused to modification of root geometry with the intention of changing the flow of WM in the root area. The modification consisted in the production of a groove at the weld root. The triangle grove was 0.3 mm high and 0.6 mm wide in the base (**Figure 1**). In the last stage, modification of processing parameters was tested, especially the shape and size of EB spot (only for X5 steel).

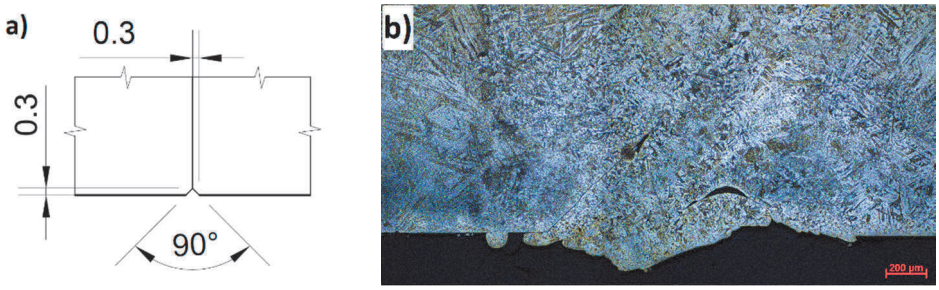

Figure 1 Root of EB welds in combination with wedge: a) diagram of groove in the root; b) sample S6

For EB welding the constant accelerating voltage was used (U_A = 120 kV). EB was focused into the half of samples thickness. The circular shape of EB spot was used on all samples with the exception of sample S7. Dimensions of used EB spot were 0.2 x 0.2 mm for samples S1 and T1 and 0.4 x 0.4 mm for the remaining samples with circular EB spot. Only on sample S7 the parabolic spot was used (X axis: 1 mm and Y axis: 0.4 mm; the X axis was in welding direction). The remaining process parameters are listed in **Table 2**.

Specimens for the metallographic analysis were ground, polished and etched in Marble (for X5 steel; 243 ml HCl; 236 ml C_2H_6O; 47.24 g $CuSO_4$) and Kroll's (for Ti64 alloy; 2 ml HF, 8 ml HNO_3, 92 ml distilled H_2O) reagents. The study of microstructures was carried out using a Zeiss Axio optical microscope and Zeiss Ultra Plus scanning electron microscope equipped with EDS Oxford Analyser.

Table 2 Parameters of EB welding

Sample	S1	S2	S3	S4	S5	S6	S7	T1	T2	T3	T4	T5
I_b (mA)	26.5	23	30	39	29	30	27	23	30	30	29	25
v (mm/s)	20	20	20	10	5	5	5	20	5	20	5	5
f (Hz)	500	500	500	500	1000	750	200	500	1000	500	1000	750
t (mm)	10	10	10	20	20	20	20	10	20	10	20	20

3. RESULTS AND DISCUSSION

In first stage the test welds were made in to the both of BM for a purpose to evaluation of their weldability (sample S1 and T1). Structure of welded sample S1 had the finer austenite grains than BM of X5 steel (**Figure 2a**). Rapid heat dissipation led to formation of low carbon martensite during solidification of molten WM. The small amount of δ-ferrite was observed at the grain boundaries of the initial austenite due to crystallization process of X5 steel (liquid → δ-ferrite + austenite → δ-ferrite + martensite). Structure of sample T1 is shown of **Figure 2b**. Microstructure of BM has lamellar morphology and consist of the plates of α phase and the residual β phase between the α plates. In the heat affected zone was observed the mixture of α plates, martensitic α' phase and unmelted β phase. The WM had a fully α' martensitic structure. The influence of process parameters on the structure of the resulted weld joints was not proven. The presence of severe weld defects was not confirmed during qualitative evaluation of weld joints. Just in the case of deep weld joints (thickness t < 8 mm; **Figure 3**), the uneven projections of WM were found in the root side due to lower surface tension of BM. Values of surface tension decrease as a result of excessive local superheating of molten metal [8].

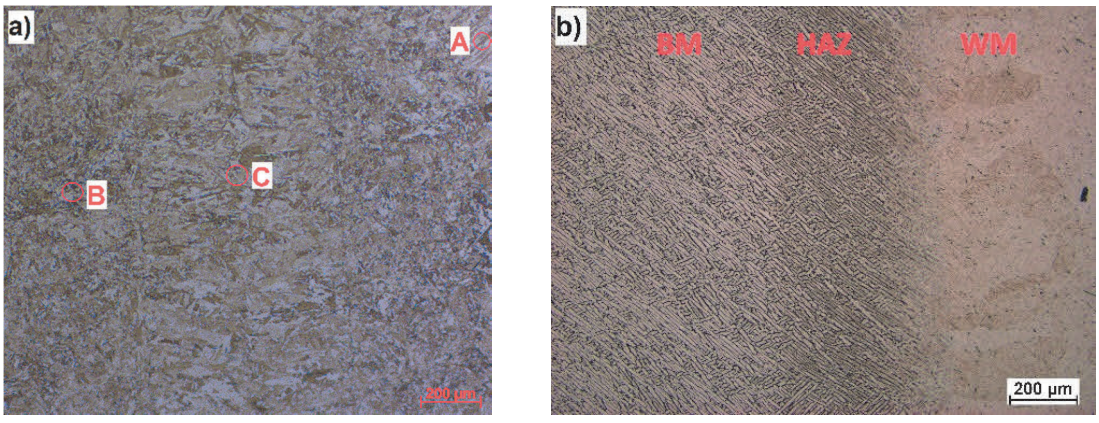

Figure 2 Structure of electron beam welds: a) X5 steel (A - base metal; B - heat affected zone; C - weld metal) and b) Ti64 alloy

During second stage was tested background material. The tungsten was used as a physical barrier to prevent of WM protrusion. Tungsten was chosen due to high melting temperature. Consequently, it was required to limited dilution of BM and tungsten background material. The parameters used for welding samples S3 and T3 led to joining of BM to background material. The background material had to be removed after EB welding which led to substandard weld root. Analysis of sample S3 by scanning electron microscopy

revealed the presence of crack and confirmed that the tungsten was mixed with the WM up to distance of 1.75 mm from the root joint (**Figure 4a**). Areas enriched with tungsten were observed in sample T3 (**Figure 4b**).

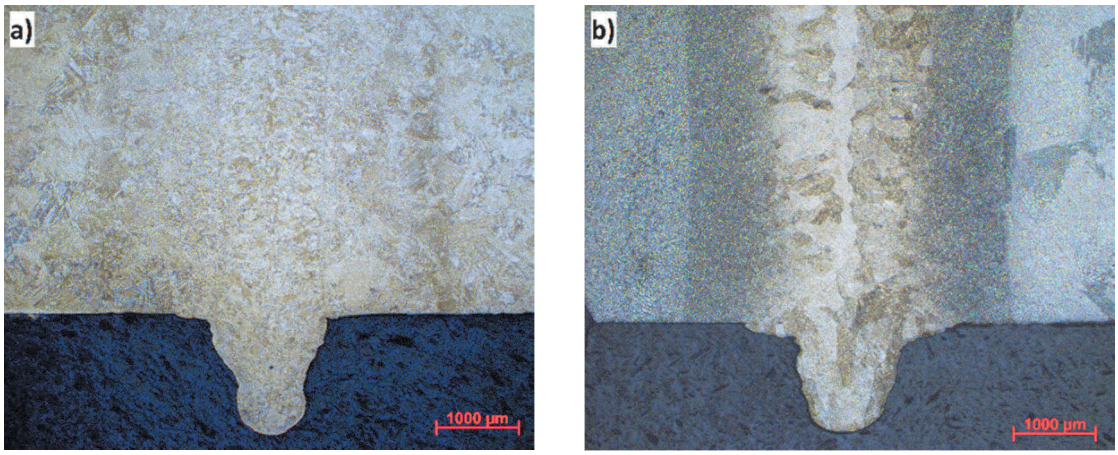

Figure 3 Root side of butt welds (t = 20 mm): a) sample S2 (height of projection 1.48 mm) and b) sample T2 (height of projection 1.33 mm)

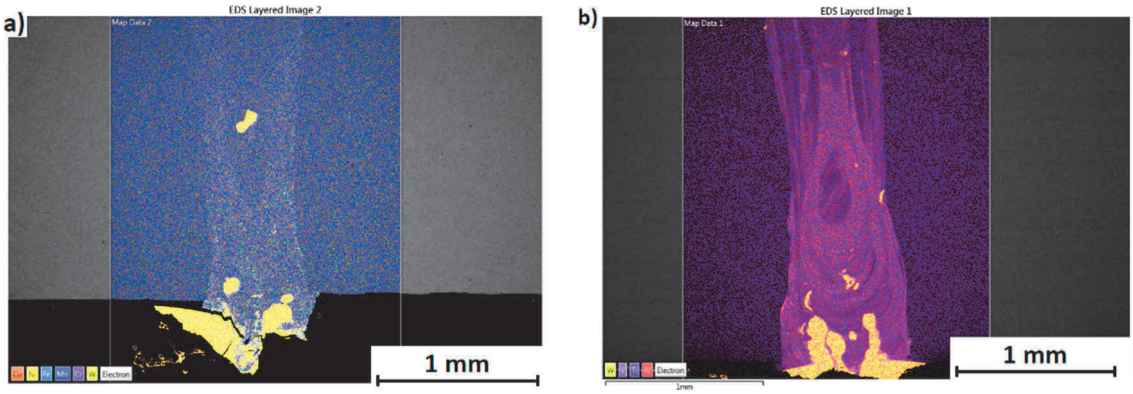

Figure 4 Root side of EB welds with background material (yellow color indicates enriched areas with tungsten): a) sample S3 and b) sample T3

Another approach was tested in experiments with nickel solder filling the root gap. The parameters set for welding of sample S4 led to undesirable interaction of EB with the solder. The high input energy level caused partial removing of the solder form the root and formation of large voids in WM (**Figure 5a**). Reducing input energy from 4.56 kW to 3.48 kW was achieved by decreasing of EB current (I_b = 38 mA → 29 mA) and thus the interaction of EB with solder was avoided. This setting resulted in the solder began melted due to the thermal conductivity of used material. The melted solder was mixed with WM and the result was the welds without large voids, but excessive protrusions of WM still occurred at the root area and in the whole weld line (**Figures 5b** and **5c**). Another defect was the presence of microcracks at the WM/solder interface.

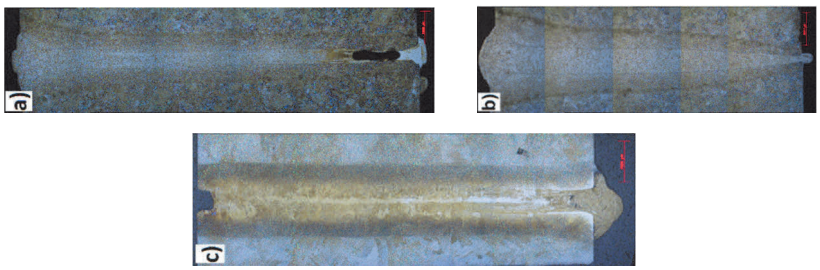

Figure 5 EB welds with solder to fill the root: a) sample S4; b) sample S5; c) sample T4

The third stage was focused to changing of WM flow by modification of weld root geometry. Artificially groove (**Figure 1a**) caused a change in the pressure conditions in the root of weld. Due to this, the influence of physical properties of used materials had manifested more markedly in comparison with previous stages. Combination of X5 steel and groove led to reduction of spiking at sample S6 (**Figure 1b**). However, cold shuts were observed on the walls of groove. When the Ti64 alloy (sample T5) was used in combination with groove, the different result was reached in comparison with sample S6. The spiking tendency did not be reduced by using the groove due to lower surface tension of the titanium alloy [8]. The appearance of root on sample T5 was similar like on sample T2 (**Figure 1b**).

In the last stage was tested the change of shape of EB spot. In previously experiments, the circular EB spot was used. The parabolic shape of EB spot was tested in order to change the energy distribution in keyhole during EB welding. In both materials the parabolic spot of EB affected the distribution of energy and thus also the flow of the molten metal [3]. A continuous head of weld was formed with a forfeited WM around 1.4 mm (**Figure 6a**). Limitation of spikes has been achieved due to parabolic shape of EB spot. On the other hand, the uneven root of weld was observed in combination with spatter of WM (**Figure 6b**). The height of weld root was varied from -0.36 mm to 0.42 mm from the total depth of weld (t = 20 mm).

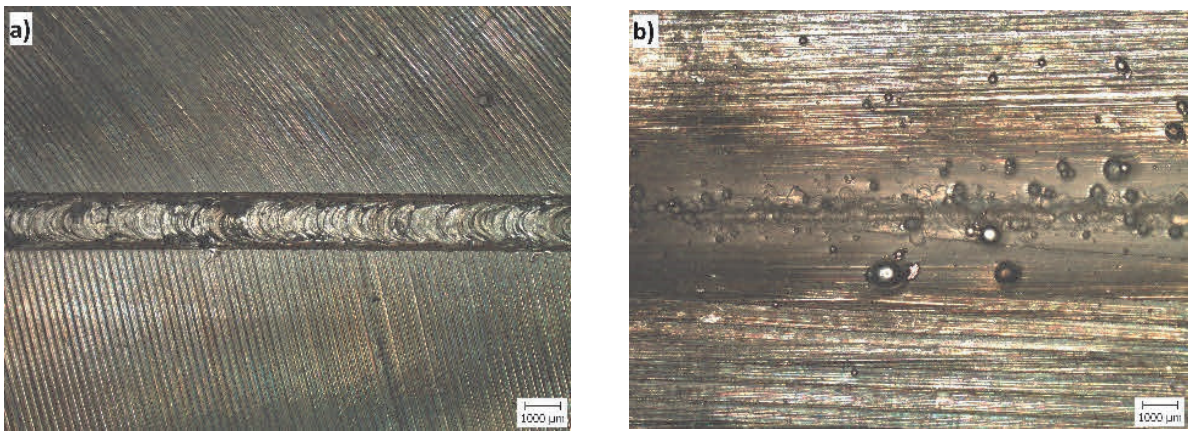

Figure 6 Sample S7: a) the head of weld; b) the root of weld

4. CONCLUSIONS

In this paper, the root stability of thick EB welds have been investigated. The main results are summarized as follows:

- Steel X5 and alloy Ti64 are easily weldable by EB welding method (without a presence of weld defects in structure). The probability of spiking formation is growing with thickness of welded material up to 8 mm.
- The background material with high melting temperature did not stop the leakage of WM in the root area. In the full penetration welds, the EB still had sufficient energy to interact with background material. It led to dilution of BM with background material that could promote cracking in the root.
- If solder was using to fill root gap is necessary to avoid interaction of EB with solder. When interaction occurred, the solder from root was removed and large void are formed in the WM. The process parameters must be set so that the solder melts due to heat dissipation from the weld. Nevertheless the excessive leakage of molten has not been prevented.
- The groove at the root of the weld changes the conditions necessary to maintain a keyhole. The influence of the physical properties of the used materials on appearance of the root was more pronounced. Spiking was limited in the case of X5 steel. However, cold shuts were observed on the groove walls. Reduction of spiking failed on Ti64 alloy due to low surface tension of molten titanium.

- Changing the shape of the EB spot caused a change in energy distribution, which resulted in a variation of the conditions inside the keyhole. The spiking was reduced by this approach. A continuous root has formed but undesirable spatter of WM was observed. This approach appears to be the most appropriate way to eliminate the spiking phenomenon.

ACKNOWLEDGEMENTS

This work has been supported by Ministry of Industry and Trade of the Czech Republic in the framework of the research project TRIO - FV10385 The advanced impeller manufacturing technology and by European Regional Development Fund in the framework of the research project NETME Centre under the Operational Program Research and Development for Innovation No. CZ.1.5/2.1.00/01.002 and within the project NETME plus (Lo1202) project of Ministry of education, Youth and Sports, under the "national sustainability programme"

REFERENCES

[1] TONG H., GIEDT W. H. A Dynamic Interpretation of Electron Beam Welding. *Welding Journal,* 1970, vol. 49, no.6, pp. 259-s-266-s.

[2] LIENERT, T. J., BABU, S. S., SIEWERT, T.A., ACOFF, V.L. eds. *ASM Handbook: Welding Fundamentals and Processes*, *vol. 6A. 1st ed.* Materials Park: ASM International, 2011, 920 p.

[3] AMSTRONG R. E. Control of Spiking in Partial Penetration Electron Beam Welds. *Welding Journal,* 1970,. vol. 49, no. 8, pp. 382-388.

[4] ARATA Y., MATSUDA F., MURAKAMI T. Some Dynamic Aspects of Weld Molten Metal in Electron Beam Welding. *Transactions of JWRI,* 1973, vol. 2, no. 2, pp. 152-161.

[5] GIEDT W. H. A periodic melting model of high intensity electron beam welding. In *Proceedings of 5th International Conference on Modeling of Casting, Welding and Advanced Solidification Processes*. Davos: MCWS Assoc., 1991, pp. 115-122.

[6] WEI P. S., CHUANG K. C., KU J. S., DEBROY T. Mechanism of Spiking and Humping in Keyhole Welding. *IEEE Transactions on Components, Packaging and Manufacturing Technologies,* 2012. vol. 2, no. 3, pp. 383-394.

[7] ČSN EN 26848 - Wolframové elektrody na svařování elektrickým obloukem v inertním plynu a plazmové řezání a svařování, 1995.

[8] SARESH N., PILLAI M. G., MATHEW J. Investigation into effects of electron beam welding on thick Ti-6Al-4V titanium alloy. *Journal of Materials Processing Technology,* 2007, vol. 192-193, pp. 83-88.